Journal of Fluorescence, Vol. 7, No. 1, 1997

Development of Long-Lifetime Metal–Ligand Probes for Biophysics and Cellular Imaging

Joseph R. Lakowicz,[1] Ewald Terpetschnig,[1] Zakir Murtaza,[1] and Henryk Szmacinski[1]

Received June 14, 1996; accepted October 15, 1996

Metal–ligand complexes containing ruthenium, osmium, or rhenium display a high photostability, with polarized emission and decay times from 100 ns to 100 μs. Such probes have considerable potential in biophysics, clinical chemistry, and fluorescence microscopy. In this review we summarize recent developments from this laboratory on the spectral properties of conjugatable metal–ligand complexes. We also suggest how improved probes can be developed based on the selection of organic ligands.

KEY WORDS: Metal–ligand probes; biophysics; cellular imaging; spectral properties.

INTRODUCTION

Time-resolved fluorescence measurements on the nanosecond time scale are now routine in many laboratories. Modern time-domain or frequency-domain instrumentation, combined with laser light sources, provides resolution of complex intensity and anisotropy decays. The applications of fluorescence are now more limited by probe chemistry than by instrumentation. In particular, most fluorophores display decay times of 1 to 10 ns. Hence, it is difficult to use fluorescence to measure biopolymer motions on a slower time scale. Additionally, the autofluorescence of biological samples, also on the nanosecond time scale, limits the sensitivity to detection of signals above the background level.

We are circumventing the limitations of short decay times by developing a new class of metal–ligand fluorophores which display decay times ranging from 100 ns to several microseconds. These complexes display useful anisotropy and, thus, can be used to measure protein hydrodynamics on the microsecond time scale. These metal–ligands are highly photostable and should thus be useful in fluorescence microscopy. We describe the present status of these probes and the possibility for advanced metal–ligand complexes with improved spectral properties. With such long-decay time probes one can imagine increased sensitivities, with off-gating of the prompt autofluorescence and simple instrumentation for lifetime-based sensing and imaging.

RESULTS

Metal–Ligand Probes for Biochemistry

In designing a fluorescence experiment one can select among thousands of fluorophores with different absorption and emission wavelengths. However, the range of available decay times is rather limited, with most decay times being in the range of 1 to 10 ns. Since a typical protein with a molecular weight of 60,000 displays a rotational correlation time near 50 ns, the 1- to 10-ns

[1] Center for Fluorescence Spectroscopy and Medical Biotechnology Center, Department of Biochemistry and Molecular Biology, University of Maryland School of Medicine, 725 West Lombard Street, Baltimore, Maryland 21201.

[2] *Abbreviations used:* MLC, metal–ligand complexes; FLIM, fluorescence lifetime imaging microscopy; HSA, human serum albumin; bpy, 2,2'-bipyridine; dcbpy, 4,4'-dicarboxy-2,2'-bipyridine; MLCT, metal-ligand charge transfer; MPE, multiphoton excitation; FRET, fluorescence resonance energy transfer; LED, light-emitting diode.

1053-0509/97/0300-0017$12.50/0

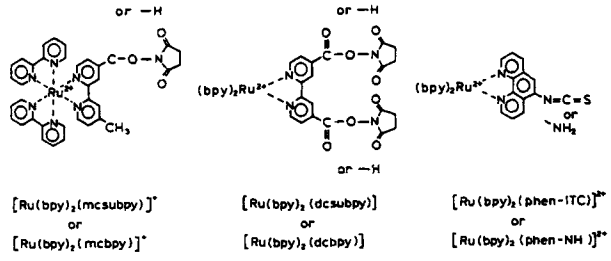

Scheme I. Chemical structure of three Ru metal–ligand probes.

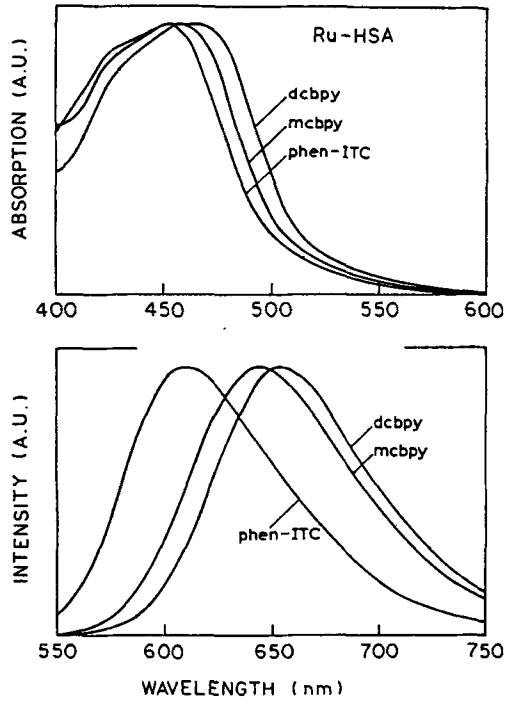

Fig. 1. Absorption and emission spectra of $[Ru(bpy)_2(dcbpy)]$, $[Ru(bpy)_2(mcbpy)]^+$, and $[Ru(bpy)_2$ phen-ITC$]^{2+}$ conjugated to HSA.

time scale is too short to study rotational or translational motion of larger macromolecules. For many biochemical experiments it would be valuable to have longer decay times, which would allow measurement of slower domain-to-domain motions in proteins, lipid diffusion in membranes, or rotational motions of membrane-bound proteins. Probes with long decay times would allow intensity and anisotropy decay measurements with relatively simple instrumentation for clinical applications. The sensitivity of the measurements can be increased by off-gating of the interfering autofluorescence. Additionally, the development of long-lived probes would allow fluorescence lifetime imaging microscopy (FLIM)[2] with simple solid-state instrumentation.

We have developed a series of conjugatable and luminescent metal–ligand complexes (MLC) which display decay times up to 1 μs,[1–3] and other molecules in this class can have decay times as long as 100 μs.[4,5] Several of these MLC probes are shown in Scheme I. The parent compound $[Ru(bpy)_3]^{2+}$ has been widely studied for use in solar energy conversion. However, such molecules have not been used as anisotropy probes. As a result of its symmetric structure, it was thought that the anisotropy of $[Ru(bpy)_3]^{2+}$ would be low and, thus, not useful for measuring the hydrodynamics of biomolecules. The anisotropy of $[Ru(bpy)_3]^{2+}$ could also be low due to exchange of energy among the identical diimine ligands. We have now found that the presence of a suitable nonidentical ligand on $[Ru(bpy)_3]^{2+}$ results in a high fundamental anisotropy. One such ligand is the dicarboxy derivative of 2,2'-bibyridyl (dcbpy) (Scheme I, center). This ligand allows coupling of $[Ru(bpy)_2(dcbpy)]$ to macromolecules by formation of a reactive *N*-hydroxy succinimide ester. MLCs have been developed which contain a isothiocyanate group for coupling with amines or a maleimide (not shown) for coupling with sulfhydral groups.[6]

It is informative to examine the absorption and emission spectra of the three MLCs shown in Scheme I. These spectra are shown in Fig. 1 for the MLCs covalently bound to human serum albumin (HSA). Important aspects of these spectral properties are the convenient excitation and emission wavelengths and the large Stokes' shift. The large Stokes' shift indicates that the probes will not be sensitive to self-quenching, as is known to occur with fluorescein-type probes. These complexes can be excited with visible wavelengths ranging from 400 to 500 nm, which are available from a variety of laser sources and even from simple and inexpensive light-emitting diodes (LEDs). The emission is shifted by nearly 200 nm, which results in easy separation of the scattered excitation and emission of the sample. The long-wavelength emission centered at 650 nm can potentially be observed in biological samples and even in whole blood. Another important property of the MLCs is their high photostability. We have had an aqueous solution $[Ru(bpy)_2(dcbpy)]$ exposed to the room light for over 2 years with no change in its absorption spectrum. This suggests that MLCs will be valuable in fluorescence microscopy, where the usual fluorophores often photobleach in seconds or minutes.

In Fig. 1, one notices that the absorption and emission maxima are longer for the carboxy derivatives than for the amino derivative. The differences observed for the absorption bands of the three complexes are smaller (15 nm) than observed for the emission maximum (45

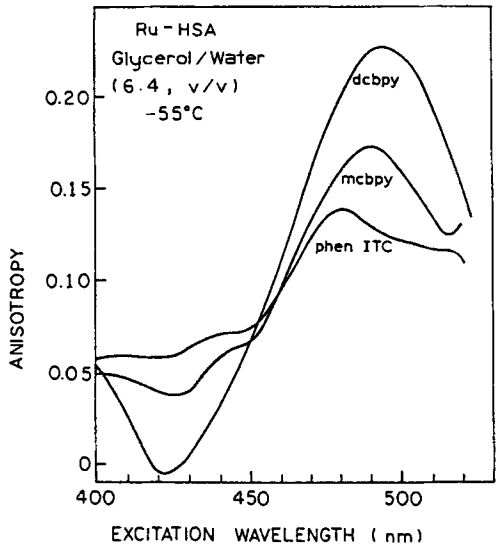

Fig. 2. Excitation anisotropy spectra of $[Ru(phen\text{-}ITC)\text{-}(bpy)_2]^{2+}$, $[Ru(dcbpy)(bpy)_2]$ and $[Ru(mcbpy)(bpy)_2]^{+}$ conjugated to HSA.

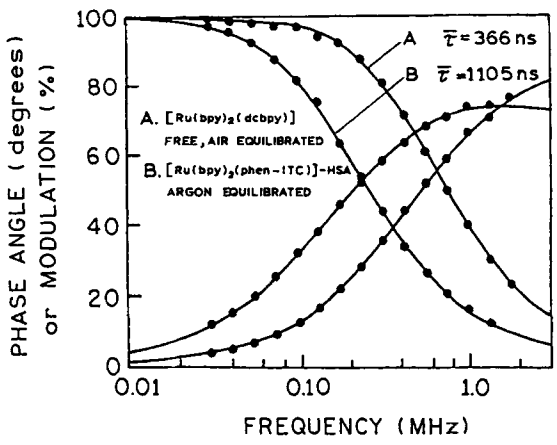

Fig. 3. Frequency-domain intensity decay of a $[Ru(bpy)_2(dcbpy)]$ free probe in air equilibrium and $[Ru(bpy)_2(phen\text{-}ITC)]$–HSA in the absence of oxygen.

nm). The excitation polarization spectra (Fig. 2) measured in frozen solutions reveal the anisotropy (r_0) of the probe in the absence of rotational diffusion. The highest value for the initial anisotropy (r_0 = 0.23) was observed for the (dcbpy)–HSA conjugate, followed by the (mcbpy) and (phen-ITC) derivatives, with r_0 values of 0.17 and 0.14, respectively. Hence it appears that a long-wavelength emission is correlated with a high fundamental anisotropy (r_0).

At present our understanding of the factors governing the anisotropy of MLCs is incomplete. However, it seems that a necessary requirement is the presence of at least one nonidentical ligand in the $M(L)_3$ complex. If one of the ligands can exist in a lower-energy metal–ligand charge transfer (MLCT) state, then the excited state can be localized between the metal and the ligand(s) with the lowest energy. A high anisotropy (r_0) is expected if there is only one nonidentical ligand with the lowest MLCT energy. This has already been supported by anisotropy measurements of $[Ru(bpy)_3]^{2+}$ and $[Ru(bpy)_2(dcbpy)]$.[2,7] Randomization of the energy among the ligands appears to be one reason why $[Ru(bpy)_3]^{2+}$ exhibits a lower r_0 value (0.15) compared to $Ru(bpy)_2(dbpy)$ (0.23).[2] The value of r_0 is strongly dependent on properties of the nonidentical ligand relative to the others.[7] The MLCT state energies of bpy and phen are sensitive to the substitution patterns and introduction of heteroatoms into their ring system. Electron-donating substituents (methyl, amino, alkylamino groups) in 4 and 4' positions of the bipyridine ring system were observed to increase the MLCT energy, and electron-withdrawing groups such as COOH, COOEt, and SO_3H are expected to lower the MLCT energy. The lower value of r_0 observed for the phen-ITC probe may be explained by similar MLCT energies of the phen-ITC and the bpy MLCT states.[7]

The maximum emission wavelength of the three complexes increases in the order phen-NH_2, mcbpy, and dcbpy; the maximum anisotropies increase in the same order. This suggests that the principles of MLCT state energy can be used to predict which metal–ligand probes will display the highest anisotropy. However, the anisotropy values of the MLCs are not completely predictable. For instance, we expected a higher r_0 value for $[Ru(mcbpy)(bpy)_2]^{1+}$ because the excited state may be localized on the carboxy side of mcbpy (Scheme I). However, the observed value of 0.17 is markedly lower than for dcbpy (0.23). This result is somewhat unexpected since the emission spectrum of $[Ru(mcbpy)(bpy)_2]^{1+}$ is much closer to that of $[Ru(dcbpy)(bpy)_2]$ than that of $[Ru(bpy)_3]^{2+}$. Evidently, the presence of two electron-withdrawing carboxyl groups provides higher localization of the MLCT state than a single carboxy group.

Another important characteristic of the MLC probes is the decay times. To date, the longest-decay time probe we have characterized is $[Ru(bpy)_2(phen\text{-}ITC)]^{2+}$ conjugated to HSA, which displays a decay time of over 1 μs (Fig. 3). The mono- and dicarboxy MLCs display decay times near 400 ns. An investigation of the effect of oxygen on the quantum yields of the free and protein bound Ru complexes showed that the sensitivity of the protein-bound form is modest and will not require elimination of oxygen. Compared to their deoxygenized so-

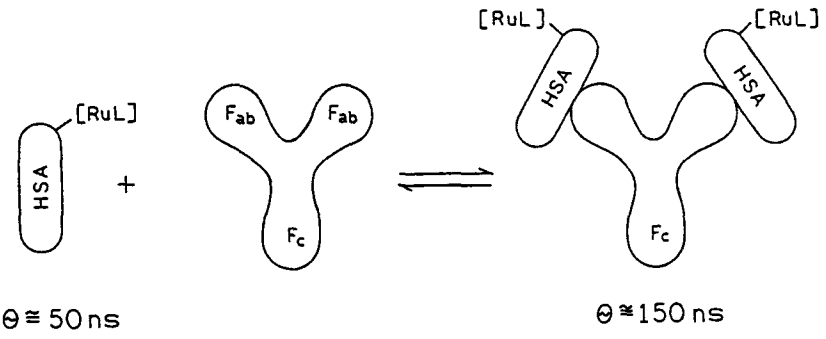

Scheme II. Effect of HSA–antibody binding on the HSA correlation time. RuL is the Ru–ligand complex, and θ is the rotational correlation time.

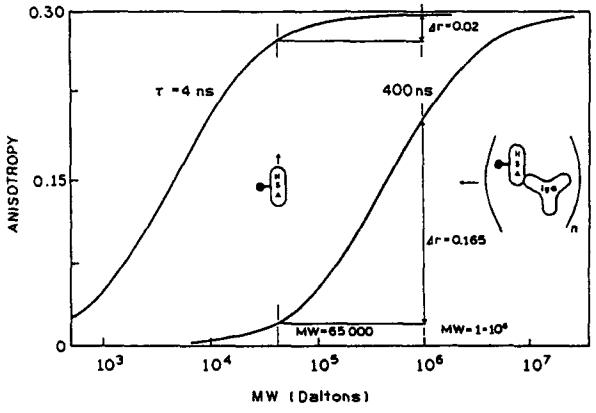

Fig. 4. Comparison of anisotropy measurement with decay times of 4 and 400 ns.

lutions, the relative fluorescence intensities for free [Ru(bpy)$_2$(dcbpy)] and the complex conjugate to HSA in air-equilibrated buffer solutions were 0.77 and 0.89, respectively. The intensity of the free Ru complex is more sensitive to dissolved oxygen than the protein-bound form.

Microsecond Rotational Motions

The advantage of long decay times is illustrated by how the anisotropy of a probe is affected by changes in molecular weight. To illustrate this point we consider how the anisotropy can be expected to change for a probe with a 4-ns lifetime conjugated to HSA (Scheme II). The rotational correlation time of HSA is near 50 ns. The steady-state anisotropy can be calculated from the Perrin equation

$$\frac{r_0}{r} = 1 + (\tau/\theta) \qquad (1)$$

where r_0 is the fundamental anisotropy, r the measured anisotropy, τ the lifetime, and θ the rotational correlation time. The expected dependence of the anisotropy or molecular weight is shown in Fig. 4. Because the correlation time of HSA is longer than the 4-ns lifetime, the emission of the 4-ns probe is almost completely polarized. Hence such a probe cannot be expected to display a significantly increased anisotropy if the protein rotation is slowed, as would occur upon binding to antibody. The anisotropy can increase by only 0.02. In contrast, if the decay time is 400 ns, then the emission of the HSA is mostly depolarized, and the anisotropy can increase by 0.165 or more upon binding to other proteins (Fig. 4). Hence, by use of probes with longer decay times, one can expect to observe slower rotational motions.

The measurement of slow rotational motions is illustrated by the frequency-domain anisotropy decays (Fig. 5) of HSA labeled with [Ru(bpy)$_2$(dcpby)] in the presence of increasing amounts of antibody to HSA. These data were analyzed globally in terms of a two-correlation time model,

$$r(t) = \sum_j r_{oj}\, e^{-t/\theta_j} \qquad (2)$$

where θ_j are the correlation times and r_{0j} the amplitudes. For the global analysis the correlation times were the global parameter since it was assumed that the two correlation times would be present in all samples: the fast component near 50 ns due to free HSA and the slow component due to the complexes of HSA with antibody. The global analysis revealed two correlation times of 36 and 5.1 μs (Table I), with the amplitudes of the slow component increasing with increased antibody concentration. These results demonstrate the possibility of measuring microsecond rotational motions with MLC probes.

It should be noted that MLC probes can also be used to study the complex hydrodynamics of DNA. Turro, Barton, and co-workers have described MLCs which display luminescence only when bound to

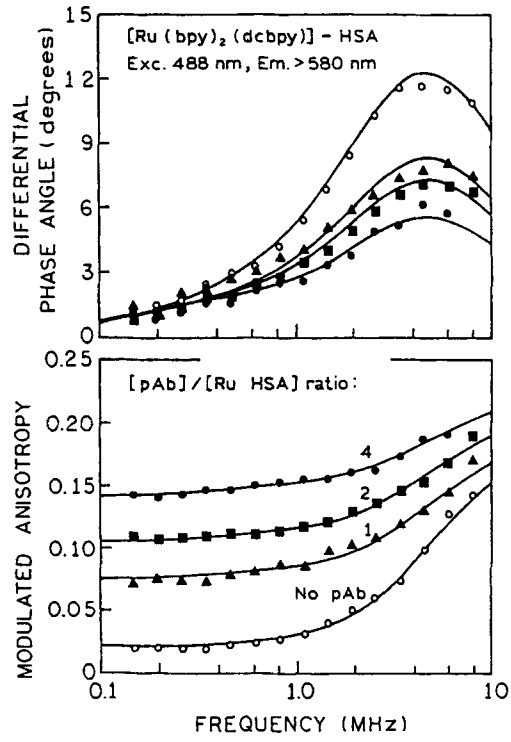

Fig. 5. Frequency-domain anisotropy decays of $Ru(bpy)_2(dcpby)$–HSA in the absence and presence of the polyclonal antibody to HSA.

Table I. Global Anisotropy Decay Analysis of [Ru(bpy)(dcbpy)] Conjugated to HSA in the Presence of Various Amounts of Antibody to HSA

Ratio Ab/Ag	$Ru(bpy)_2(dcbpy)$–HSA (θ_1 = 36 ns; θ_2 = 5115 ns)		
	r_{01}	r_{02}	Σr_{0i}
0	0.173	0.008	0.181
1.0	0.117	0.072	0.189
2.0	0.103	0:105	0.208
4.0	0.078	0.145	0.223
8.0	0.086	0.140	0.226

DNA.[8,9] The chemical structure of one such complex is shown in Scheme III. An advantage of this type of probe is that it is essentially nonfluorescent in water and becomes highly fluorescent when bound to DNA. The mode of binding is apparently intercalation of the dppz ligand between the base pairs of double-helical DNA. Contact of the nitrogen atoms in dppz with water results in quenching, and such contact is prevented when bound to DNA. This result suggests that it is possible to develop environmentally sensitive MLC probes, analogous to the widely used DNS and ANS fluorophores. We have

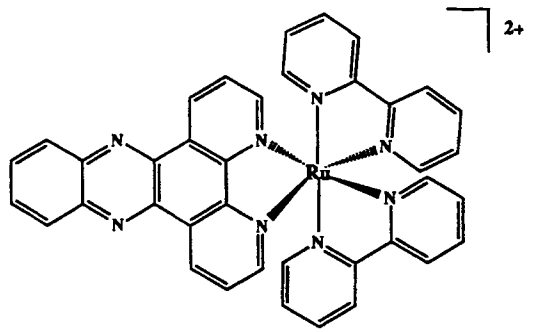

Scheme III. Chemical structure of a DNA anisotropy probe, $Ru(bpy)_2(dppz)$.

shown that the emission from $[Ru(bpy)_2(dppz)]^{2+}$ is polarized and can be used to measure DNA dynamics.[10] Such measurements can be used to test the available theories for the bending and twisting motions of DNA.[11,12]

Domain Motions in Proteins

In addition to rotational diffusion, the long-lifetime MLC probes can be useful for studies of translational diffusive processes on a time scale presently not accessible with the usual fluorescence probes. For instance, there is considerable interest in the rates and amplitudes of domain-to-domain motions in proteins,[13] and there have been repeated attempts to study such motions by time-resolved fluorescence resonance energy transfer (FRET).[14–16] These measurements have been mostly unsuccessful because of the 5- to 10-ns decay times and the limited extent of interdomain motions on this time scale. The use of longer-lived MLC emission can allow measurements of these motions. This possibility is illustrated in Fig. 6, which shows the effect of site-to-site motions on the frequency-domain intensity decay of donors with decay times of 2 and 200 ns. The assumed diffusion coefficient of 10^{-7} cm²/s is comparable to that one can expect for such motions. Such slow diffusion has no significant effect on the intensity decay of the 2-ns probe (Fig. 6, top), and hence the intensity decay cannot be used to measure the diffusion coefficient. In contrast, diffusion has a significant effect on the intensity decay of the 200-ns probe (Fig. 6, bottom) as is shown by the shaded area. The effect of diffusion is to increase the extent of energy transfer and thus decrease the donor decay time. Since MLC probes with longer microsecond decay times are likely to be available soon, one can anticipate measuring diffusion rates of 10^{-8}–10^{-9} cm²/s. We have now detected FRET for a MLC donor in a

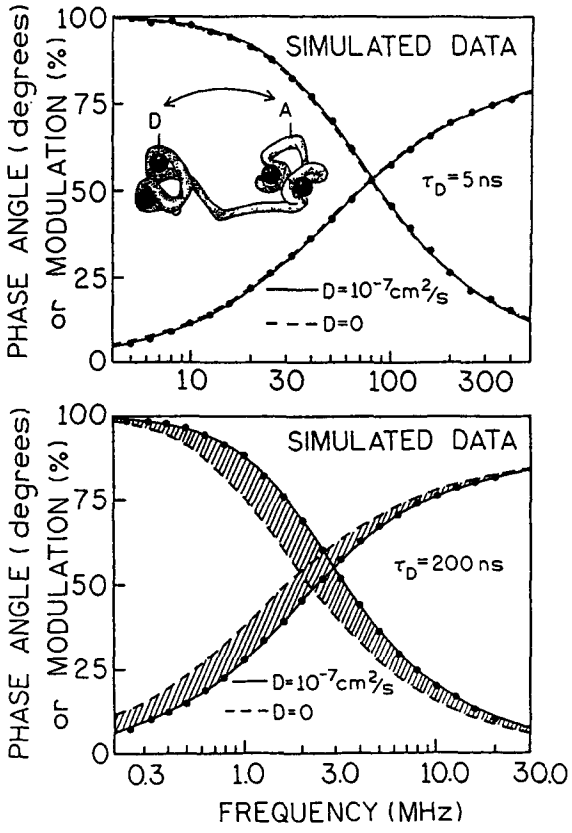

Fig. 6. Possibility of measuring domain motions in proteins with long-lifetime probes.

donor–acceptor pair,[17] so that one can expect measurements of domain motions to follow soon. We note that such measurements are not the equivalent of diffusion-enhanced energy transfer using the lanthanide donors, in which the rate of diffusion is not determined, and the data reveal only the distance of closest approach of the donor and acceptor.

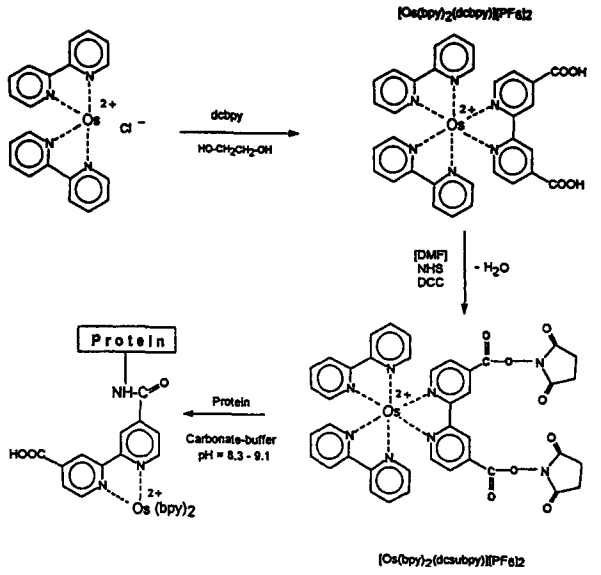

Scheme IV. Synthesis of a reactive osmium metal–ligand complex.

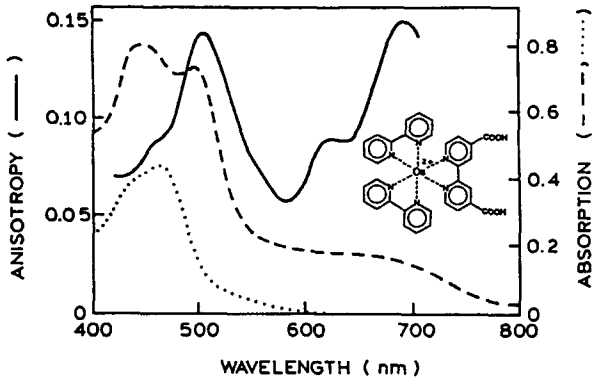

Fig. 7. Absorption (—) and excitation anisotropy spectra (— — —) of $[Os(bpy)_2(dcbpy)]^{2+}$. The dotted line shows the absorption spectrum of $[Ru(bpy)(dcbpy)]^{2+}$.

Advanced MLC Probes

The sensitivity of fluorescent measurements in biological samples, especially for clinical testing, is determined by the amount of background fluorescence from the samples. Background fluorescence (background scattered light and fluorescence signals from endogenous sample components) is highly reduced at longer wavelengths beyond 650 nm. Additionally, probes absorbing near 650 nm allow the use of laser diode light sources. Hence we synthesized[18] an Os analogue of the dicarboxy Ru complex, $[Os(bpy)_2(dcbpy)]$ (Scheme IV). This Os complex exhibits long-wavelength absorption up to 700 nm (Fig. 7) and an emission maximum at 750 nm (Fig. 8). The complex was activated and coupled to a protein. Importantly, there are two maxima in the excitation anisotropy spectrum (Fig. 8), one at 505 nm and one at 685 nm. The high anisotropy value at 685 nm of 0.14 is ideal for tracing protein interactions using a 690-nm diode laser, though the lifetime of the Os complex is short (19 ns).

Osmium complexes with longer lifetimes, in the range of a few hundred nanoseconds can be obtained by replacing the bpy ligands with tppz [tetrakis-(pyridyl)pyrazine], which should allow the measurement of longer correlation times using diode laser excitation. For instance, we have synthesized two such fluorophores

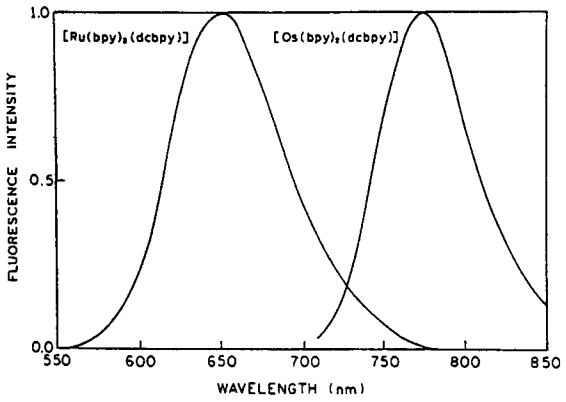

Fig. 8. Emission spectra of $Ru(bpy)_2(dcpby)$ and $Os(bpy)_2(dcbpy)$.

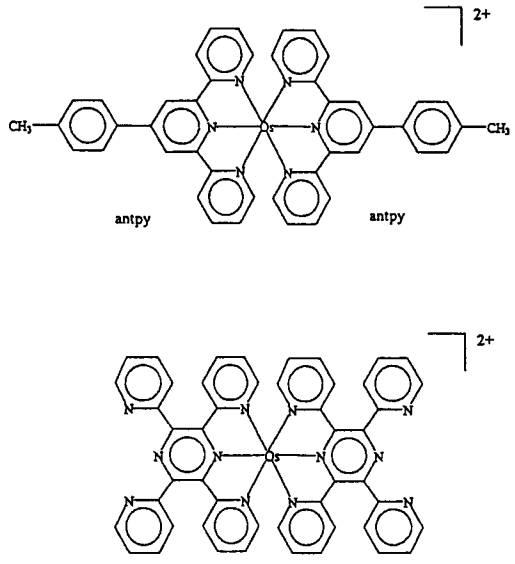

Scheme V. Long-lifetime laser diode-excitable osmium complexes.

(Scheme V). Both osmium complexes can be excited at 680 nm. $Os(antbpy)_2$ displays a decay time of 200 ns in deoxygenated methanol, and $Os(tppz)_2$ a decay time of 175 ns. Hence it is possible to obtain both long decay times and long—wavelength absorption using Os complexes. A disadvantage of the complexes shown in Scheme V are the low quantum yields of the Os complexes. This problem can be circumvented by using arsine or phosphine ligands.[19,20] One such complex synthesized in this laboratory is shown in Fig. 9. In acetonitrile this complex displays a quantum yield of 0.4 and a decay time of 2.3 μs (Fig. 10). The lifetime remains long in water, 1.43 μs (Fig. 10). While the dppy ligand is rather hydrophobic, a sulfonated dppy ligand is commercially available. Hence, MLC probes can be made with high quantum yields and lifetimes. However,

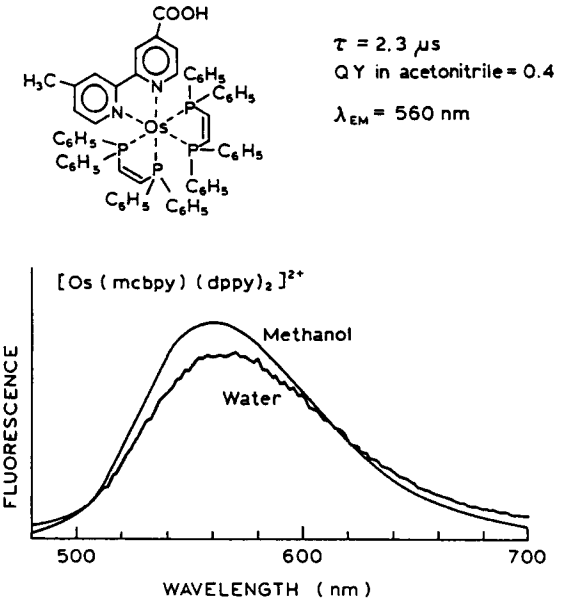

Fig. 9. Structure and emission spectrum of a high-quantum yield Os complex.

the use of arsine or phosphine ligands results in spectral properties similar to those of the Ru complexes.

The use of arsine and phosphine ligands can be extended to include DNA probes. Two such potential structures are shown in Scheme VI. Based on previous literature one can expect these probes to display quantum yields near 0.4 and decay times of several microseconds. Synthesis and characterization of structures similar to those in Scheme VI are in progress.

Re-Based MLCs with Millisecond Lifetimes and High Quantum Yields

Extremely long lifetimes and high quantum yields are characteristic of some Re(I)-based metal complexes.[21] The isonitrile derivatives $(L)Re(CO)_3C = NR$ (L = phen, bpy; $R = n - Bu$, $t - Bu$) of such Re-MLC have excited-state lifetimes in the range of hundreds of microseconds and quantum yields of >0.7 at room temperature in aqueous solutions.[21] These properties make them very attractive for applications as sensors or molecular probes. Demas and co-workers have recently described the synthesis and spectral properties of rhenium (Re) MLCs.[22] When such complexes contain an isonitrile ligand the quantum yields are near 0.8 and the decay times as long as 100 μs. Surprisingly, the long-lived isonitrile derivatives are reported to be stable in alcohol and aqueous solutions.[22] Other reports have also described highly fluorescent and long-lived Re com-

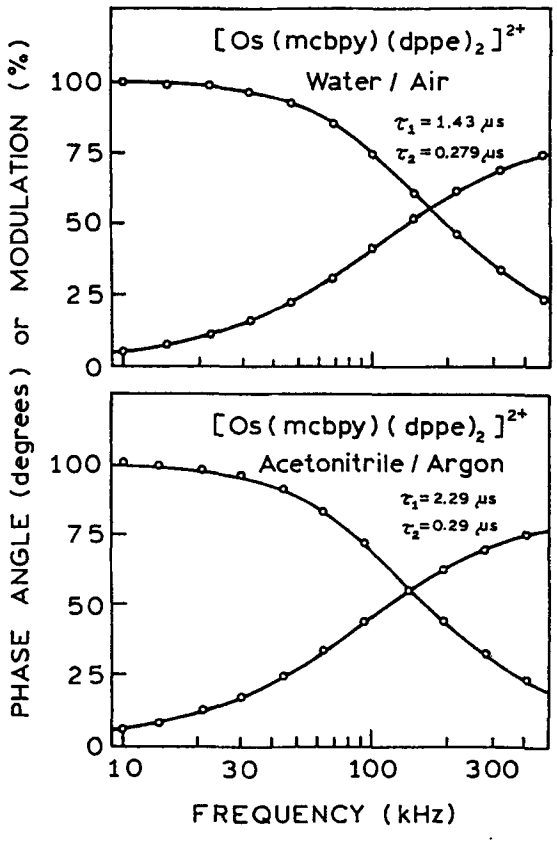

Fig. 10. Frequency-domain intensity decays of $[Os(mcbpy)(dppe)_2]^{2+}$.

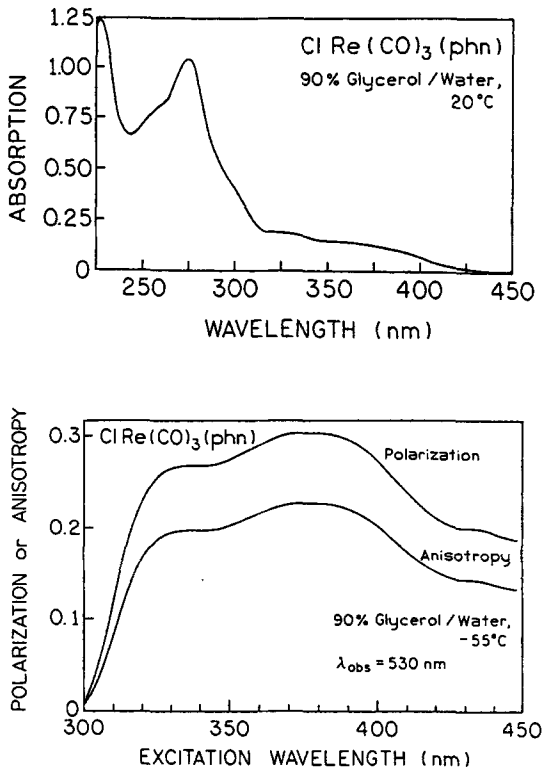

Fig. 11. Absorption (top) and excitation anisotropy spectrum (bottom) of $ClRe(CO)_3(phn)$.

Highly Luminescent Probes for DNA

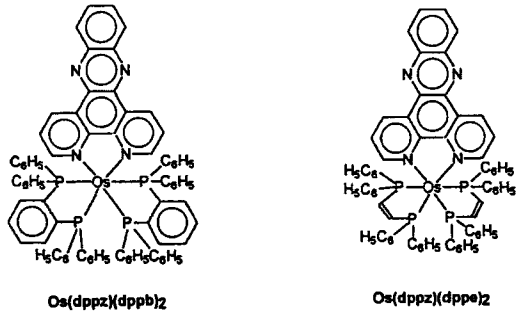

Scheme VI. Potential high-quantum yield DNA probes.

plexes.[21-24] One obvious application for long-lived Re complexes is gated detection following decay of the prompt autofluorescence from biological samples. Gated detection is widely used with the long-lived lanthanides, especially in immunoassays.[25] Another application could be in fluorescence polarization immunoassays, assuming that the Re complexes display polarized emission. The excitation polarization spectrum of Cl–$Re(CO)_3$(phen) is shown in Fig. 11 (bottom) and reveals high polarization values for this compound.[26] These preliminary anisotropy studies illustrate the potential of the Re complexes as high-quantum yield biophysical probes.

One disadvantage of the Re probe is the short-wavelength absorption spectra (Fig. 11, top). However, this is now less of a problem because of the development of UV-emitting LEDs,[27] and the possibility of blue laser diodes.[28]

DISCUSSION

In the past several years we have demonstrated the possibility of cellular imaging based on the fluorescence lifetime or decay time at each point in the image,[29,30] a method now referred to as fluorescence lifetime imaging microscopy (FLIM). As presently accomplished, FLIM requires a light source modulated near 100 MHz and a high-speed gain-modulated image intensifier. These requirements can be eliminated using long-lived MLC probes. It is now known that the output of LEDs can be

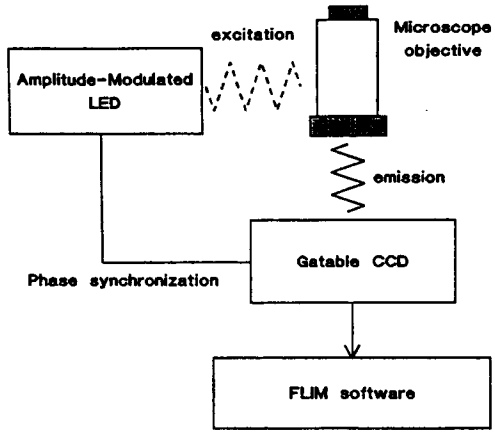

Scheme VII. Fluorescence lifetime imaging microscopy (FLIM) with long-lived probes. The excitation can be an amplitude-modulated LED and the emission detected with a gatable CCD.

modulated at frequencies up to 50 MHz.[31] The output of blue LEDs is well matched to the absorption spectra of the Ru metal–ligand complexes. Importantly, CCDs are becoming available with gated detection near 50 ns.[32] Such detectors would allow collection of the phase-sensitive images for FLIM without an image intensifier (Scheme VII). Hence, the instrumentation for FLIM can be rather simple, and the use of a LED light source and photostable MLCs may minimize problems of photobleaching. The capabilities for FLIM may then become a routine part of a fluorescence microscope.

ACKNOWLEDGMENTS

The concepts and results described in this article were developed over a number of years. Dr. Joseph R. Lakowicz wishes to thank the National Institutes of Health (RR-08119, RR-10416, GM-39617, GM-35154) and the National Science Foundation (MCB-8804931, BIR-9319032, DIR-8710401) for their continued support.

REFERENCES

1. E. Terpetschnig, H. Szmacinski, and J. R. Lakowicz (1995) *Anal. Biochem.* **227**, 140–147.
2. E. Terpetschnig, H. Szmacinski, H. Malak, and J. R. Lakowicz (1995) *Biophys. J.* **68**, 342–350.
3. H. Szmacinski, E. Terpetschnig, and J. R. Lakowicz (1996) *Biophys. Chem.* **62**(1–3), 109–120.
4. J. N. Demas and B. A. DeGraff (1992) *Macromol. Chem. Macromol. Symp.* **59**, 35–51.
5. L. A. Sacksteder, M. Lee, J. N. Demas, and B. A. DeGraff (1993) *J. Am. Chem. Soc.* **115**, 8230–8238.
6. E. Terpetschnig, J. D. Dattelbaum, H. Szmacinski, and J. R. Lakowicz (1996) *Anal. Biochem.* (submitted).
7. B. A. DeGraff and J. N. Demas (1994) *J. Phys. Chem.* **98**, 12478–12480.
8. A. E. Friedman, J.-C. Chambron, J. P. Sauvage, N. J. Turro, and J. K. Barton (1990) *J. Am. Chem. Soc.* **112**, 4960–4962.
9. R. M. Hartshorn and J. K. Barton (1992) *J. Am. Chem. Soc.* **114**, 5919–5925.
10. J. R. Lakowicz, H. Malak, I. Gryczynski, F. N. Castellano, and G. J. Meyer (1995) *Biospectroscopy* **1**, 163–168.
11. J. M. Schurr, B. S. Fujimoto, P. Wu, and L. Song (1992) in J. R. Lakowicz (Ed.) *Topics in Fluorescence Spectroscopy, Vol. 3. Biochemical Applications*, Plenum Press, New York, pp. 137–229.
12. M. D. Barkley and B. H. Zimm (1979) *J. Chem. Phys.* **70**, 2991–3007.
13. M. Gerstein, A. M. Lesk, and C. Chothia (1994) *Biochemistry* **33**(22), 6737–6749.
14. G. Haran, E. Haas, B. K. Szpikowska, and M. T. Mas (1992) *Proc. Natl. Acad. Sci. USA* **89**, 11764–11768.
15. P. S. Eis, J. Kuśba, M. L. Johnson, and J. R. Lakowicz (1993) *J. Fluoresc.* **3**, 23–31.
16. J. R. Lakowicz, I. Gryczynski, J. Kuśba, W. Wiczk, H. Szmacinski, and M. L. Johnson (1994) *Photochem. Photobiol.* **59**(1), 16–29.
17. H. J. Youn, E. Terpetschnig, H. Szmacinski, and J. R. Lakowicz (1995) *Anal. Biochem.* **232**, 24–30.
18. E. Terpetschnig, H. Szmacinski, and J. R. Lakowicz (1996) *Anal. Biochem.* **240**, 54–59.
19. R. G. Brewer, G. E. Jensen, and K. J. Brewer (1994) *Inorg. Chem.* **33**, 124–129.
20. C. R. Arana and H. O. Abruna (1993) *Inorg. Chem.* **32**, 194–203.
21. L. A. Sacksteder, M. Lee, J. N. Demas, and B. A. DeGraff (1993) *J. Am. Chem. Soc.* **115**, 8320–8238.
22. T. G. Kotch, A. J. Lees, S. J. Fuerniss, K. I. Papathomas, and R. W. Snyder (1993) *Inorg. Chem.* **32**, 2570–2575.
23. R. J. Shaver, D. P. Rillema, and C. Woods (1990) *J. Chem. Soc.*, 179–180.
24. G. A. Retiz, J. N. Demas, B. A. Degraff, and E. M. Stephens (1988) *J. Am. Chem. Soc.* **110**, 5051–5059.
25. E. P. Diamandis (1988) *Clin. Biochem.* **21**, 139–150.
26. J. R. Lakowicz, J. Murtaza, W. E. Jones, K. Kim, and H. Szmacinski (1996) *J. Fluoresc.* **6**(4), 245–249.
27. T. Araki and H. Misawa (1995) *Rev. Sci. Instrum.* **66**(12), 5469–5472.
28. G. Fasoi (1996) *Science* **272**, 1751–1752.
29. J. R. Lakowicz, H. Szmacinski, K. Nowaczyk, K. Berndt, and M. L. Johnson (1992) *Anal. Biochem.* **202**, 316–330.
30. J. R. Lakowicz, H. Szmacinski, K. Nowaczyk, W. J. Lederer, and M. L. Johnson (1994) *Cell Calcium* **15**, 7–27.
31. S. Fantini, M. A. Franceschini, J. B. Fishkin, B. Barbieri, and E. Gratton (1994) *Appl. Opt.* **33**(22), 5204–5213.
32. K. K. Reich, R. W. Mountain, W. H. McGonagle, C. M. Huang, J. C. Twichell, B. B. Kosicki, and D. Savoye (1991) *Proc. IEEE* **91**, 721–724.